

# Kinetic Treatment of Irreversible Cyclooligomerization of Bifunctional Chains and Its Relevance to the Synthesis of Many-Membered Rings<sup>1</sup>

Gianfranco Ercolani,\* Luigi Mandolini,\* and Paolo Mencarelli\*

Dipartimento di Chimica and Centro C.N.R. di Studio sui Meccanismi di Reazione, Università di Roma "La Sapienza", I-00185 Roma, Italy. Received August 18, 1987

**ABSTRACT:** The reaction of a bifunctional reactant A-B under batchwise conditions to give macrocycles has been simulated by numerical integration of the proper system of differential rate equations. This was set up considering all the possible processes of concurrent cyclization and polymerization up to a polymerization degree of 12. In order to obtain meaningful yield data for the cyclooligomers, realistic sets of effective molarities (EM) have been considered. The results show how the yields of the various cyclooligomers vary as a function of the initial monomer concentration and provide useful guidelines to achieve maximum selectivity in the synthesis of a given ring. It is clearly shown that the yield of any cyclooligomer is a function of the whole set of EM values. This observation is the basis of a procedure here developed to evaluate EM data from experimental yields of cyclooligomers. Merits and limitations of more simplified kinetic schemes, which had been previously suggested, are discussed in light of the present results.

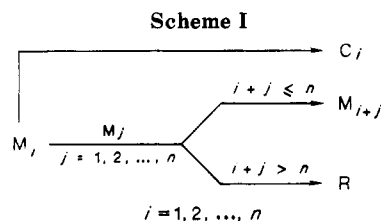
Long-chain bifunctional molecules of the type A-B can undergo macrocyclization or stepwise polymerization, depending upon the reaction conditions. In principle, it is always possible to carry out cyclization at monomer concentrations low enough so as to render polymerization negligible. In actual cases, however, macrocyclization reactions are often run under conditions where extensive polymerization takes place.<sup>2</sup> It is useful, therefore, to consider a general kinetic treatment of the case where the bifunctional reactant undergoes simultaneous cyclization and polymerization. Such a system is described by a kinetic scheme where a countless number of competitive as well as competitive-consecutive reactions render the analytical solution a hopeless task. Approximate solutions are available<sup>3-5</sup> with varying degrees of applicability, depending on the reaction conditions.<sup>6</sup> A major limitation of these approximate treatments is that no information whatever is obtained as to the effect of dilution and other parameters on yields of cyclic oligomeric species, i.e., cyclic dimer, trimer, etc., the formation of which is often significant in cases of practical interest.

We now describe a more refined approximate treatment, where the formation of both linear and cyclic oligomers with polymerization degree up to 12 is taken into account. The procedure involves the microcomputer-assisted numerical integration of the proper system of differential rate equations by the simple Euler method.<sup>7</sup>

## Kinetic Treatment

Consider a bifunctional chain molecule A-B, where A and B are two different functional groups each capable of reacting irreversibly with the other only. In the kinetics of polymerization the reactivity of a functional group is assumed to be independent of the size of the molecule to which it is attached.<sup>8</sup> Deviations from this rule are known,<sup>9</sup> which are bound to the existence of poorly understood effects associated with the chain length. The matter is closely related to the conceptual difficulties met in the operational definition of inherent reactivity of functional groups to be used in quantitative investigations of intramolecular reactions for the calculation of the effective molarity (EM).<sup>6,10</sup> The EM is defined by the ratio  $k_{\text{intra}}/k_{\text{inter}}$ , where  $k_{\text{intra}}$  is the specific rate for cyclization and  $k_{\text{inter}}$  refers to an arbitrarily chosen intermolecular model reaction.

In spite of the above difficulties, the usual assumption of functional group reactivity independent of chain length



will be used throughout the present work. Any possible inaccuracy deriving therefrom is largely offset by greater simplicity and generality. It is worth noting that, by virtue of the above assumption, any distinction disappears between the EM and Stoll's cyclization constant  $C = k_{\text{intra}}/k_{\text{dim}}$ , where  $k_{\text{dim}}$  is the specific rate for dimerization of A-B.<sup>3</sup>

Let us now consider the reaction system outlined in Scheme I, where  $M_i$  and  $C_i$  represent the open chain and cyclic  $i$ -meric oligomer, respectively.

The stepwise polymerization is arbitrarily truncated at the  $n$ -mer, in that when  $i + j \leq n$  any reaction between  $M_i$  and  $M_j$  leads to a product  $M_{i+j}$  which is still capable of propagating the reaction sequence, whereas when  $i + j > n$  the product R (residual polymer) is considered unreactive. This is equivalent to the assumption that when R is formed the concentration of unreacted end groups is so low that cyclization of R largely predominates over further stepwise polymerization. Accordingly, the complete set of differential equations describing the concentration changes of the whole family of cyclic and open chain oligomers up to the  $n$ -mers is formulated as

$$d[C_i]/dt = (k_{\text{intra}})_i[M_i] \quad i = 1, 2, \dots, n \quad (1)$$

$$-d[M_1]/dt = (k_{\text{intra}})_1[M_1] + 2k_{\text{inter}}[M_1]^2 + 2k_{\text{inter}}[M_1] \sum_{j=2}^n [M_j] = (k_{\text{intra}})_1[M_1] + 2k_{\text{inter}}[M_1] \sum_{j=1}^n [M_j] \quad (2)$$

$$-d[M_2]/dt = (k_{\text{intra}})_2[M_2] - k_{\text{inter}}[M_1]^2 + 2k_{\text{inter}}[M_2] \sum_{j=1}^n [M_j] \quad (3)$$

$$-d[M_3]/dt = (k_{\text{intra}})_3[M_3] - 2k_{\text{inter}}[M_1][M_2] + 2k_{\text{inter}}[M_3] \sum_{j=1}^n [M_j] \quad (4)$$

$$-d[M_4]/dt = (k_{\text{intra}})_4[M_4] - k_{\text{inter}}[M_2]^2 - 2k_{\text{inter}}[M_1][M_3] + 2k_{\text{inter}}[M_4]\sum_{j=1}^n[M_j] \quad (5)$$

or in general

$$-d[M_i]/dt = (k_{\text{intra}})_i[M_i] - k_{\text{inter}}\sum_{j=1}^{i-1}[M_j][M_{i-j}] + 2k_{\text{inter}}[M_i]\sum_{j=1}^n[M_j] \quad i = 1, 2, \dots, n \quad (6)$$

There is a subtle question in the derivation of the above differential rate equations bound to the presence of the coefficient 2 in some of the terms related to stepwise polymerization and not in others, which deserves a comment. Referring, for example, to eq 2, the coefficient 2 preceding  $k_{\text{inter}}[M_1]^2$  simply means that two  $M_1$  species disappear upon dimerization, but that preceding the crossed products  $[M_i][M_j]$  with  $j \neq 1$  is due to the fact that the specific rate of the reaction between two different bifunctional molecules is  $2k_{\text{inter}}$ . This can be shown as follows. Let us react a mixture of two different bifunctional reactants  $M_i$  and  $M_j$ . In terms of functional group concentrations  $[-A] = [-B] = [M_i] + [M_j]$ , the reaction rate of the intermolecular processes  $v_{\text{inter}} = -d[A]/dt = -d[B]/dt$  is written as

$$v_{\text{inter}} = k_{\text{inter}}[-A][-B] = k_{\text{inter}}([M_i] + [M_j])^2 = k_{\text{inter}}[M_i]^2 + k_{\text{inter}}[M_j]^2 + 2k_{\text{inter}}[M_i][M_j] \quad (7)$$

The quadratic terms refer to the two dimerization processes, whereas the last term refers to the crossed reaction, the specific rate of which is clearly twice as great as that of dimerization. This is because the crossed reaction is actually the sum of two independent reactions, namely, the reaction of the A end of  $M_i$  with the B end of  $M_j$ , and vice versa. The two reactions lead to the same product but proceed through different transition states.

It is convenient, for our purposes, to divide the set of eq 1 and 6 by a dimensionless constant  $f$  having the same numerical value of  $k_{\text{inter}}$ . This operation changes the time scale ( $t' = ft$ ) and makes the terms  $(k_{\text{intra}})_i$  and  $k_{\text{inter}}$  numerically equal to  $EM_i$  and 1, respectively, without changing their dimensions. Therefore the set of eq 1 and 6 simplifies to the following equations:

$$d[C_i]/dt' = EM_i[M_i] \quad i = 1, 2, \dots, n \quad (8)$$

$$-d[M_i]/dt' = EM_i[M_i] - \sum_{j=1}^{i-1}[M_j][M_{i-j}] + 2[M_i]\sum_{j=1}^n[M_j] \quad i = 1, 2, \dots, n \quad (9)$$

In order for the results of the simulated experiments to be meaningful, realistic values of the  $EM_i$  parameters are to be used in the calculations. For the sake of concreteness, let us consider a bifunctional chain leading to a medium ring with, say, 10 ring atoms, so that  $C_2$  is 20-membered,  $C_3$  30-membered, and so on. It is well-known that the  $EM$ 's in the medium ring region vary significantly,<sup>6,11</sup> depending upon the structure of the ring being formed. For ring size 20, there is observed a much lesser dependence on structure, most of the available  $EM$  values related to the formation of rings in the neighborhood of 20 skeletal atoms being well included in the fairly limited range of 0.01–0.1 M. On the other hand, the ease of closure of large rings is found, as would be expected, to be independent of the chemical nature of the end groups, which is equivalent to saying that the  $EM$ 's for very large rings are solely determined by the conformational entropy change upon cyclization.<sup>6</sup> Accordingly,  $EM$  values from  $EM_3$  (30-mem-

**Table I**  
EM Values in mol L<sup>-1</sup> Related to the Formation of Oligomeric Rings  $C_i$  with  $i = 2, 3, \dots, 12$

ring size	$i$	$EM_i, M^a$	ring size	$i$	$EM_i, M^a$
20	2	0.030	80	8	0.0088
30	3	0.038	90	9	0.0074
40	4	0.025	100	10	0.0065
50	5	0.018	110	11	0.0057
60	6	0.014	120	12	0.0051
70	7	0.011			

<sup>a</sup>  $EM_i$  values with  $i = 3, 4, \dots, 12$  are calculated from eq 10. For  $EM_2$  see text.

bered ring) onward were calculated from eq 10, where  $N_A$  is Avogadro's number, and  $EM$  is expressed in moles per liter when  $r$  is given in centimeters.<sup>12,13</sup>

$$EM = \frac{1000}{N_A} \left( \frac{3}{2\pi \langle r^2 \rangle} \right)^{3/2} \quad (10)$$

The mean-square chain end displacement  $\langle r^2 \rangle$  is related to the number  $x$  and length  $b$  of skeletal bonds through eq 11, where  $C_x$  is the characteristic ratio.<sup>13</sup>

$$\langle r^2 \rangle = C_x x b^2 \quad (11)$$

Apart from the case of the 20-membered ring, the  $EM_i$  values listed in Table I were calculated by using a value of  $C_x \approx C_\infty = 8$ , which was found to account well for the cyclization behavior of long-chain polymethylene and poly(oxyethylene) compounds in  $Me_2SO$ .<sup>6</sup> The average value of 0.03 M was assigned to the dimeric 20-membered ring. For  $EM_1$ , the typical values of 0.0001, 0.001, 0.01, and 0.05 M were used in separate sets of simulated experiments. These were carried out according to the batchwise procedure, in which  $m$  moles of bifunctional reactant  $M_1$  are added all at once into a volume  $V$  of solvent, where the proper conditions are set. At zero time the batchwise experiment is characterized by  $[M_1]_0 = m/V$ , the concentration of all other species being zero.

## Procedure

All calculations were carried out in double precision (i.e., numbers are considered with 16 significant digits) on a IBM PC-XT computer upgraded with a 8087 coprocessor. The system of differential rate equations (8) and (9) with  $n = 12$  was numerically integrated by an ad hoc computer program based on the Euler method.<sup>7</sup> The program, written in Basic, was compiled with the IBM-Microsoft Basic Compiler ver. 2.00.

The Euler method was the method of choice because, owing to the large number of differential equations of the system under consideration, its implementation was simpler than that of more efficient but more elaborate methods.

The system of differential rate equations was integrated from the time zero to the time  $t'$  when condition (12) is verified, i.e., until the total concentration of the unreacted open chain molecules  $M_i$  expressed as weight percent was less than 0.5%. Since the

$$100 \sum_{i=1}^{12} i[M_i]_t / [M_1]_0 \leq 0.5 \quad (12)$$

Euler method is a stepwise procedure, it requires the subdivision of the total reaction time into a number of small intervals, and in general the greater this number the greater the accuracy of the results. Since, in our case, the results are expressed as percent yields, we required computational errors  $\leq 0.05$ . To obtain such accuracy the numerical integration was carried out with ca.  $10^4$  steps. Each computer run required about 45 min.

## Results

We considered four sets of simulated batchwise experiments, characterized by  $EM_1$  values equal to 0.0001, 0.001, 0.01, and 0.05 M, all the other  $EM$ 's being from Table I. Each set is composed by seven kinetic runs, each run re-

**Table II**  
Cyclooligomer Percent Yields and % R When  $EM_1 = 0.0001$  M for Selected Initial Monomer Concentrations<sup>a</sup>

	[M] <sub>1,0</sub> , M						
	0.001	0.002	0.005	0.01	0.02	0.05	0.1
C1	14.6	8.7	4.1	2.2	1.1		
C2	80.7	82.6	77.5	67.8	54.2	33.7	20.8
C3	4.0	7.4	14.3	20.0	23.7	22.2	17.2
C4			2.7	5.7	9.3	11.8	10.5
C5				2.1	4.7	7.6	7.5
C6					2.6	5.4	5.8
C7					1.5	3.9	4.7
C8						3.0	3.8
C9						2.3	3.3
C10						1.8	2.9
C11						1.5	2.5
C12						1.2	2.2
R						4.8	18.2

<sup>a</sup> Values lower than 1% are not reported.

**Table III**  
Cyclooligomer Percent Yields and % R When  $EM_1 = 0.001$  M for Selected Initial Monomer Concentrations<sup>a</sup>

	[M] <sub>1,0</sub> , M						
	0.001	0.002	0.005	0.01	0.02	0.05	0.1
C1	54.1	39.1	22.6	13.7	7.7	3.2	1.5
C2	43.0	54.4	61.6	58.8	49.5	32.2	20.4
C3	2.3	5.3	12.1	18.3	22.6	21.8	17.1
C4			2.3	5.2	9.0	11.7	10.5
C5				1.9	4.4	7.5	7.5
C6					2.5	5.3	5.8
C7					1.5	3.9	4.6
C8						2.9	3.8
C9						2.3	3.2
C10						1.8	2.8
C11						1.4	2.5
C12						1.1	2.2
R						4.5	17.7

<sup>a</sup> Values lower than 1% are not reported.

ferring to a different value of the initial monomer concentration ( $[M]_0 = 1 \times 10^{-3}$ ,  $2 \times 10^{-3}$ ,  $5 \times 10^{-3}$ ,  $1 \times 10^{-2}$ ,  $2 \times 10^{-2}$ ,  $5 \times 10^{-2}$ , 0.1 M). Concentrations lower than  $10^{-3}$  M are clearly of no practical interest. On the other hand, concentrations higher than 0.1 M are to be avoided when rings of relatively low molecular weight are desired.

Numerical integration of the proper system of differential equations for each run (see Procedure) afforded the final concentrations for all of the cyclooligomers considered ( $[C_i]$  with  $i = 1, 2, \dots, 12$ ), and from these concentrations the cyclooligomer yields, expressed in terms of weight percent, were calculated according to eq 13. The cyclo-

$$\% C_i = 100i[C_i]_{\infty}/[M]_0 \quad (13)$$

oligomer yields are reported in Tables II–V for  $i = 1, 2, \dots, 12$  and in Figure 1 for  $i = 1, 2, \dots, 5$ . The amount of residual polymer, percent R, defined as the weight percent of oligomers  $M_{i+j}$  with  $i + j > 12$  was calculated by eq 14,

$$\% R = 99.5 - \sum_{i=1}^{12} \% C_i \quad (14)$$

where the 99.5 is due to the fact that the reaction was considered complete when the condition of eq 12 is verified. % R values are also shown in Tables II–V. The value of % R is a useful indicator of the goodness of the approximate kinetic Scheme I in the explored range of initial  $M_1$  concentrations. Since the residual polymer R is considered unreactive, thus implying that its presence has no influence on the reaction course, a necessary prerequisite for the essential correctness of the treatment is that % R is sufficiently low. The greatest value obtained for % R

**Table IV**  
Cyclooligomer Percent Yields and % R When  $EM_1 = 0.01$  M for Selected Initial Monomer Concentrations<sup>a</sup>

	[M] <sub>1,0</sub> , M						
	0.001	0.002	0.005	0.01	0.02	0.05	0.1
C1	90.5	83.2	67.5	51.8	35.8	18.7	10.2
C2	8.6	14.9	26.0	33.1	34.8	27.5	18.9
C3		1.3	5.0	10.4	16.4	19.3	16.3
C4				2.8	6.4	10.4	10.1
C5					3.0	6.6	7.2
C6					1.5	4.5	5.5
C7						3.2	4.4
C8						2.3	3.5
C9						1.7	2.9
C10						1.2	2.5
C11							2.1
C12							1.8
R						2.6	14.2

<sup>a</sup> Values lower than 1% are not reported.

**Table V**  
Cyclooligomer Percent Yields and % R When  $EM_1 = 0.05$  M for Selected Initial Monomer Concentrations<sup>a</sup>

	[M] <sub>1,0</sub> , M						
	0.001	0.002	0.005	0.01	0.02	0.05	0.1
C1	97.6	95.8	90.7	83.1	71.0	49.1	32.3
C2	1.8	3.5	7.8	13.1	18.8	21.1	16.9
C3				2.7	6.7	12.9	13.6
C4					2.1	6.7	8.5
C5						3.8	5.8
C6						2.3	4.3
C7						1.4	3.2
C8							2.5
C9							2.0
C10							1.6
C11							1.3
C12							1.0
R							6.5

<sup>a</sup> Values lower than 1% are not reported.

(18.2) refers, as expected, to the kinetic experiment characterized by the lowest value of  $EM_1$  and the highest value of  $[M]_0$  ( $1 \times 10^{-4}$  M and 0.1 M, respectively). We wish to remark that even this seemingly high value of % R does not invalidate our calculations. In fact since R represents the acyclic oligomers with a number of monomer units in the range of 13–24, the corresponding end functional group percentage is necessarily lower than (% R)/13. Therefore in the worst case under consideration the approximate scheme only neglects the influence of much less than 1.4% of the reactive functional groups. Furthermore, since % R becomes significant only during the late stages of the reaction, i.e., when the concentration of unreacted functional groups is very low, a major fraction of the residual polymer R, if allowed to react, would yield unreactive cyclooligomers. Thus, a % R as large as 18.2% has but a negligible influence on the reaction course.

By inspection of Tables II–V it appears that though the “up to 12 terms” kinetic scheme is well adequate to account for initial monomer concentrations as high as 0.1 M, on increasing further  $[M]_0$  the number of terms to be included in the kinetic scheme for a correct description of the system steeply increases. It is apparent as well that at the lower  $[M]_0$  values, kinetic schemes with  $n$  lower than 12 would be equally satisfying.

## Discussion

The principal aim of the present calculations is to show how the initial monomer concentration affects, for typical EM sets, the cyclooligomer monomer concentration affects, for typical EM sets, the cyclooligomer distribution. This

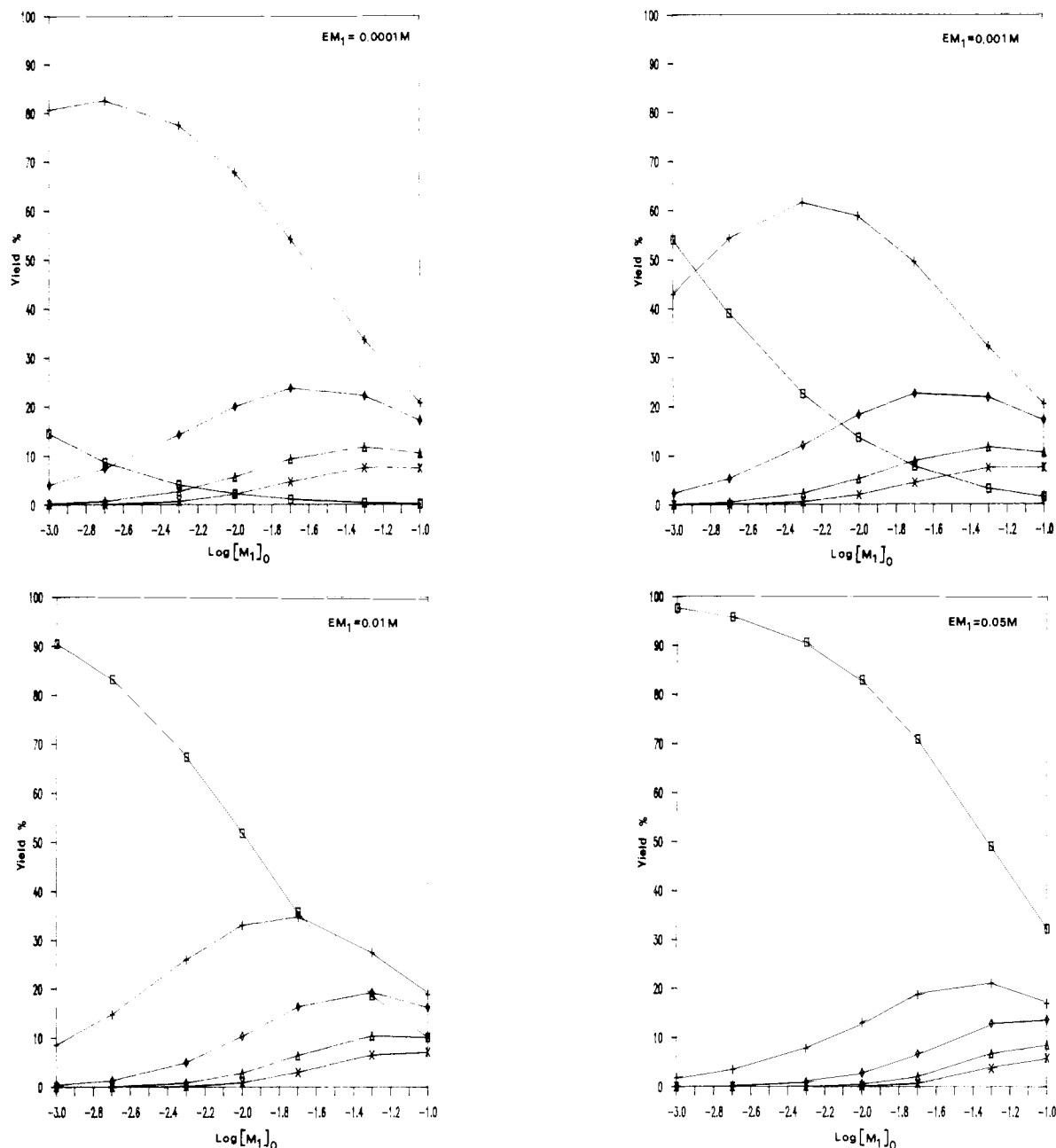
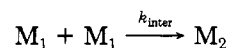
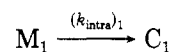


**Figure 1.** Yields of  $C_1$  ( $\square$ ),  $C_2$  ( $+$ ),  $C_3$  ( $\diamond$ ),  $C_4$  ( $\Delta$ ), and  $C_5$  ( $\times$ ) as a function of the initial monomer concentration:  $EM_1 = 0.0001$ ,  $0.001$ ,  $0.01$ , and  $0.05$  M.

is shown in Figure 1 for the cyclooligomers in the range of one to five monomer units. The figure shows a basic difference between the  $C_1$  curve and those referring to the other rings. In fact while the  $C_1$  curve monotonically decreases on increasing  $[M_1]_0$ , the other ones go through a maximum. It appears that, for the given sets of  $EM$  values, on increasing the ring size the curves become smoother and smoother, in particular their maxima decrease and are reached at higher  $[M_1]_0$  values. This behavior implies that on increasing  $[M_1]_0$  an increasing number of cyclooligomers are formed with low and comparable yields. Therefore the reaction is synthetically useful only at low  $[M_1]_0$  values and only for the lowest cyclooligomers. Clearly, the monomeric ring  $C_1$  is formed in good yield when  $[M_1]_0 < EM_1$ , and the dimeric ring  $C_2$  can be selectively obtained in the fairly good yield of about 50% or more whenever  $EM_1$  is low, i.e., less than  $10^{-3}$  M, and  $[M_1]_0$  does not exceed  $10^{-2}$  M. It is of interest to compare the yields of  $C_1$  obtained according to the present simulation experiments with the corresponding values provided by previous approximate

treatments. In the approximate solution proposed by Galli and Mandolini (Scheme II),<sup>5</sup> the stepwise polymerization

#### Scheme II



is truncated at the second step. Scheme II, which is equal to Scheme I with  $n = 1$ , implicitly assumes that the fate of the open chain dimer  $M_2$  is to cyclize to  $C_2$ . From Scheme II, eq 15 is easily obtained,

$$d[C_1] = - \frac{(k_{\text{intra}})_1}{(k_{\text{intra}})_1 + 2k_{\text{inter}}[M_1]} d[M_1] \quad (15)$$

which on integration between the limits  $[M_1] = [M_1]_0$  and  $[M_1] = [M_1]_\infty = 0$  gives

$$\% C_1 = \frac{50}{\alpha} \ln(1 + 2\alpha) \quad (16)$$

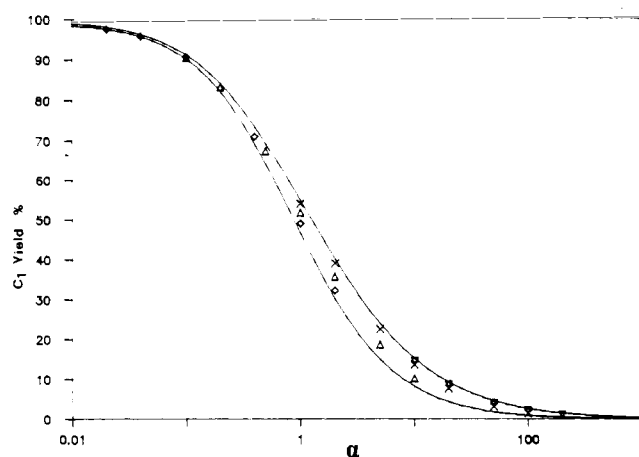
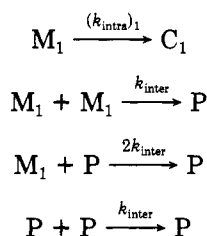


**Figure 2.** Yield of  $C_1$  as a function of  $\alpha$ . The upper curve refers to Scheme II and the lower one to Scheme III. The points in the plot, reported in Table VI, are from this work:  $EM_1 = 0.0001$  M ( $\nabla$ );  $EM_1 = 0.001$  M ( $\times$ );  $EM_1 = 0.01$  M ( $\Delta$ );  $EM_1 = 0.05$  M ( $\diamond$ ).

where  $\alpha$ , defined as  $[M_1]_0/EM_1$ , may be viewed as a reduced initial concentration.

In the treatment of Morawetz and Goodman<sup>4</sup> (Scheme III) the possible formation of polymeric ring products  $C_i$  with  $i > 1$  is totally neglected.<sup>14</sup> Here P represents any

#### Scheme III



open chain polymeric material. The set of the differential rate equations (17)–(19) corresponding to Scheme III was

$$d[C_1]/dt' = EM_1[M_1] \quad (17)$$

$$-d[M_1]/dt' = EM_1[M_1] + 2[M_1]^2 + 2[M_1][P] \quad (18)$$

$$-d[P]/dt' = [P]^2 - [M_1]^2 \quad (19)$$

numerically integrated in the present work.<sup>15</sup> The results predicted by the above approximate treatments are reported in Figure 2 as plots of  $C_1$  percent yield against the dimensionless parameter  $\alpha$ . The two curves are practically superposed when  $\alpha$  is low but differ significantly in the region of large  $\alpha$ 's, where polymerization predominates over cyclization to  $C_1$ . It has been pointed out that  $C_1$  yields are overestimated by Scheme II and underestimated by Scheme III.<sup>6</sup> This prediction is totally fulfilled by the  $C_1$  yields from Tables II–V, which are found (Figure 2) to lie invariably in the region between the two curves. This is more accurately shown by the figures listed in Table VI.

Earlier attempts at developing kinetic treatments of simultaneous macrocyclization and polycondensation were mainly aimed at calculating the  $EM_1$  value from the experimentally determined yield of  $C_1$  when the reaction is allowed to go to completion.<sup>3,4</sup> If the yield of  $C_1$  only is taken into consideration, one must necessarily refer to the oversimplified models of Scheme II and III, which can only provide, with the aid of the two sigmoid-shaped plots in Figure 2, an interval of  $EM_1$  values, given by the horizontal distance between the two curves. It is apparent that such an interval is acceptably narrow when the yield of  $C_1$  is high but becomes too wide to be meaningful in the region of low yields.

**Table VI**  
 **$C_1$  Percent Yields Calculated According to Scheme II and III Models and from This Work as a Function of  $\alpha$**

$\alpha$	Scheme II	Scheme III	$C_1$ yields, %			
			Table II	Table III	Table IV	Table V
0.02	98.1	97.5				97.6
0.04	96.2	95.6				95.8
0.10	91.2	90.2			90.5	90.7
0.20	84.1	82.1			83.2	83.1
0.40	73.5	69.2				71.0
0.50	69.3	64.1			67.5	
1.00	54.9	46.7		54.1	51.8	49.1
2.00	40.2	30.3		39.1	35.8	32.3
5.00	24.0	15.0		22.6	18.7	
10.00	15.2	8.2	14.6	13.7	10.2	
20.00	9.3	4.3	8.7	7.7		
50.00	4.6	1.8	4.1	3.2		
100.00	2.7	0.9	2.2	1.5		
200.00	1.5	0.5	1.1			

The present work has clearly shown that the yield of  $C_1$  is not only a function of  $[M_1]_0$  and  $EM_1$  but also of the EM values of the higher oligomers. More generally, the yield of any cyclooligomer is a function of  $[M_1]_0$  and of the whole set of EM values. We now propose a procedure, according to which a consistent set of EM values can be obtained from the experimental yields of a series of cyclooligomers obtained under certain experimental conditions. Let us assume that for the given experimental conditions, Scheme I with  $n = 12$  is a good representation of the real system. In this case the relationship between the EM values and the corresponding experimental yields is obtained by (i) formal integration of the system of differential equations (8), to give eq 20, (ii) substitution of eq 20 into the corresponding eq 13, and (iii) rearrangement of the resulting equations in the desired form (21) in which %  $C_i$  is the experimental yield of the  $i$ -meric ring. In order to obtain

$$[C_i] = EM_i \int_0^\infty [M_i] dt' \quad i = 1, 2, \dots, n \quad (20)$$

$$EM_i = (\% C_i)[M_1]_0 / \left( 100i \int_0^\infty [M_i] dt' \right) \quad (21)$$

$EM_i$  we must be able to evaluate the integral in the corresponding eq 21. Since  $[M_i]$  is in turn function of all the EM values we suggest an iterative procedure which starts from trial EM values and takes into account all of eq 21 simultaneously. A reasonable set of trial EM values can be obtained from Figure 2 for  $C_1$  and by eq 10 for the other rings. Having chosen the trial EM set, the numerical evaluation of all the  $[M_i]$  integrals is straightforward. According to eq 20, we can evaluate these integrals by dividing  $[C_i]$ , calculated with the trial EM set, by the trial  $EM_i$  value. By substitution of the numerical value of the integrals so obtained in eq 21, a better set of EM values is obtained. We can use these new values for a more accurate evaluation of the  $[M_i]$  integrals and so on until the EM set remains unchanged. It seems likely that in most cases of practical interest precise yield data can possibly be obtained for  $C_1$  and  $C_2$  only. Therefore in such cases we must consider only eq 21 with  $i = 1, 2$ . It is obvious that the EM values of the other cyclooligomers cannot be optimized and one should rely on the initial choice of the EM values for these rings. This is unlikely, however, to cause significant errors on the estimate of the  $EM_1$  and the  $EM_2$  values. Regrettably we are not aware of experimental yield data precise enough to test the accuracy of the method with respect to kinetically obtained EM values. However, the correctness of the procedure has been checked by using as experimental yields for  $C_1$  and  $C_2$  some

of the values reported in Tables II-V. Starting with trial EM<sub>1</sub> and EM<sub>2</sub> values rather different from those which generated the above yields, we succeeded in reproducing the correct EM<sub>1</sub> and EM<sub>2</sub> values.

### Concluding Remarks

As stressed in a previous paper in this series,<sup>16</sup> we believe that in a large number of available reports on the synthesis of many-membered rings, the physicochemical fundamentals underlying ring closure are either ignored or applied incorrectly and that many current interpretations in the field are based on concepts whose mechanistic feasibility still awaits substantiation. A major difficulty undoubtedly arises from the kinetic complexity of systems where extensive polymerization competes with macrocyclization. In order to fill the gap between the general physicoorganic foundation of intramolecular reaction and the synthetic strategies for ring closure, a sound kinetic background is needed. We have now shown that this problem can be satisfactorily solved by means of a computational procedure involving the computer aided numerical integration of the complex system of differential equations, coupled with meaningful sets of EM values. These are derived from the accumulation in recent years of extensive quantitative studies in the field,<sup>6,10,11,17</sup> which have put the dilution principle into proper perspective.

In the present work various cyclization reactions involving bifunctional reactants A-B (one-component ring closure) have been simulated under batchwise conditions. The results nicely show the way the various parameters determine the outcome of a given cyclization reaction in terms of distribution among cyclic oligomers. Hopefully, they can provide the synthetic chemist with useful guidelines to achieve maximum selectivity in a desired cyclooligomer.

For the sake of a close adherence of calculations to actual experimental procedures, current work is devoted to simulation of one-component ring closure under influxion conditions, i.e., under conditions where the bifunctional

reactant is added slowly into the reaction medium<sup>2</sup> (Ziegler's high dilution conditions). Similarly, simulation of two-components ring closure,<sup>18,19</sup> i.e., A-A + B-B, is under current investigation under both batchwise and influxion conditions.

**Acknowledgment.** Financial support by the Ministero della Pubblica Istruzione, Rome, is greatly acknowledged.

### References and Notes

- (1) Part 26 of the series "Ring-Closure Reactions". Part 25: Casadei, M. A.; Di Martino, A.; Galli, C.; Mandolini, L. *Gazz. Chim. Ital.* **1986**, *116*, 659.
- (2) Rossa, L.; Vögtle, F. *Top. Curr. Chem.* **1983**, *113*, 1.
- (3) Stoll, M.; Rouvè, A.; Stoll-Comte, G. *Helv. Chim. Acta.* **1934**, *17*, 1289.
- (4) Morawetz, H.; Goodman, N. *Macromolecules* **1970**, *3*, 699.
- (5) Galli, C.; Mandolini, L. *Gazz. Chim. Ital.* **1975**, *105*, 367.
- (6) Mandolini, L. *Adv. Phys. Org. Chem.* **1986**, *22*, 1.
- (7) For the numerical integration of rate equations by Euler method, see Ercolani and Mencarelli (Ercolani, G.; Mencarelli, P. *Educ. Chem.* **1986**, *23*, 176).
- (8) Flory, P. J. *Chem. Rev.* **1949**, *39*, 137.
- (9) Galli, C.; Mandolini, L. *J. Chem. Soc., Perkin Trans. 2* **1977**, 443.
- (10) Kirby, A. *Adv. Phys. Org. Chem.* **1980**, *17*, 183.
- (11) Illuminati, G.; Mandolini, L. *Acc. Chem. Res.* **1981**, *14*, 95.
- (12) Morawetz, H. *Macromolecules in Solution*; Wiley: New York, 1975.
- (13) Flory, P. J. *Statistical Mechanics of Chain Molecules*; Wiley: New York, 1969.
- (14) Scheme III differs from that originally proposed by Morawetz and Goodman for the presence of the coefficient 2 in the crossed reaction M<sub>1</sub> + P (cf. the discussion on the statistical coefficient 2 in the section "Kinetic Treatment").
- (15) For the sake of convenience the solutions obtained by numerical integration can be interpolated in the range of  $\alpha$  0.01-1000 by the third-order polynomial % C<sub>1</sub> = -0.059 + 18.029 $\alpha$  + 30.499 $\alpha^2$  - 7.289 $\alpha^3$ , where  $\alpha = (\ln(1 + 2\alpha))/\alpha$ , with a standard deviation = 0.128.
- (16) Galli, C.; Mandolini, L. *J. Chem. Soc., Chem. Commun.* **1982**, 251.
- (17) Winnik, M. A. *Chem. Rev.* **1981**, *81*, 491.
- (18) Hammerschmidt, E.; Schutter, H.; Vögtle, F. *J. Chem. Res., Synop.* **1980**, 86; *J. Chem. Res., Miniprint* **1980**, 1083.
- (19) Fastrez, J. *Tetrahedron Lett.* **1987**, *28*, 419.

## Synthesis and Characterization of [<sup>13</sup>C]Lignins

Robert E. Botto

Chemistry Division, Argonne National Laboratory, 9700 South Cass Avenue, Argonne, Illinois 60439. Received July 29, 1987

**ABSTRACT:** Synthetic lignins were prepared from coniferyl alcohols, 3-(4-hydroxy-3-methoxyphenyl)propenols, specifically enriched with the <sup>13</sup>C isotope at the  $\beta$ -position in the propyl side chain or at the methoxyl carbon. A convenient synthetic route was developed to prepare reasonably large quantities (1-3 g) of [<sup>13</sup>C]coniferyl alcohols in good yields using fairly inexpensive reagents. Chemical characterization of the synthetic polymers by spectroscopic methods (solid NMR, FTIR, MS) showed some of the similarities and differences in their structure to that of natural softwood lignins.

Synthetic lignins (termed DHP's, dehydrogenative polymerizates) were first prepared by Freudenberg and his associates<sup>1-3</sup> by enzyme-controlled oxidative coupling of coniferyl alcohol. These synthetic polymers have shown some resemblance to naturally occurring softwood lignins, containing largely the same structural features of the natural materials, but not necessarily in identical proportions.<sup>4</sup> The subsequent use of synthetic lignins having radioisotopic (<sup>14</sup>C) labels incorporated at specific sites has

proved to be an extremely valuable tool for elucidating lignin structure and biosynthetic pathways<sup>5</sup> and for quantifying lignin biodegradation processes.<sup>6</sup> The more recent application of <sup>13</sup>C-labeling techniques combined with NMR spectroscopy<sup>7-9</sup> came as a natural extension of the earlier radioisotope methods.

Our interest in "polymer models" for natural lignins arises from their potential use in <sup>13</sup>C-labeling experiments to examine chemical transformations of lignin during